

This work was written as part of one of the author's official duties as an Employee of the United States Government and is therefore a work of the United States Government. In accordance with 17 U.S.C. 105, no copyright protection is available for such works under U.S. Law. Access to this work was provided by the University of Maryland, Baltimore County (UMBC) ScholarWorks@UMBC digital repository on the Maryland Shared Open Access (MD-SOAR) platform.

Please provide feedback Please support the ScholarWorks@UMBC repository by emailing scholarworks-group@umbc.edu and telling us what having access to this work means to you and why it's important to you. Thank you.

Existence conditions for phononic frequency combs

Cite as: Appl. Phys. Lett. **117**, 183503 (2020); <https://doi.org/10.1063/5.0025314>

Submitted: 14 August 2020 . Accepted: 22 October 2020 . Published Online: 05 November 2020

 Zhen Qi,  Curtis R. Menyuk,  Jason J. Gorman, and  Adarsh Ganesan



View Online



Export Citation



CrossMark

ARTICLES YOU MAY BE INTERESTED IN

An extremely anisotropic phononic crystal with open elliptical dispersion for energy convergence and beam squeezing

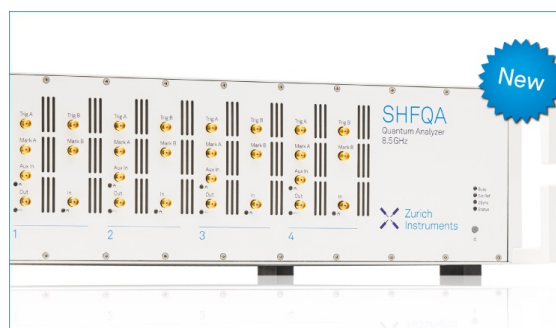
Applied Physics Letters **117**, 183501 (2020); <https://doi.org/10.1063/5.0017302>

A Perspective on acoustical tweezers—devices, forces, and biomedical applications

Applied Physics Letters **117**, 180501 (2020); <https://doi.org/10.1063/5.0028443>

Spin-orbit torques in structures with asymmetric dusting layers

Applied Physics Letters **117**, 182403 (2020); <https://doi.org/10.1063/5.0029347>



Your Qubits. Measured.

Meet the next generation of quantum analyzers

- Readout for up to 64 qubits
- Operation at up to 8.5 GHz, mixer-calibration-free
- Signal optimization with minimal latency

Find out more



Existence conditions for phononic frequency combs

Cite as: Appl. Phys. Lett. **117**, 183503 (2020); doi: [10.1063/5.0025314](https://doi.org/10.1063/5.0025314)

Submitted: 14 August 2020 · Accepted: 22 October 2020 ·

Published Online: 5 November 2020







View Online



Export Citation



CrossMark

Zhen Qi,¹  Curtis R. Menyuk,¹  Jason J. Gorman,²  and Adarsh Ganesan^{2,a)} 

AFFILIATIONS

¹Department of Computer Science and Electrical Engineering, University of Maryland, Baltimore County, Baltimore, Maryland 21250, USA

²National Institute of Standards and Technology, Gaithersburg, Maryland 20899, USA

^{a)}Author to whom correspondence should be addressed: adarshvganesan@gmail.com

ABSTRACT

The mechanical analog of optical frequency combs, phononic frequency combs, has recently been demonstrated in mechanical resonators and has been attributed to coupling between multiple phonon modes. This paper investigates the influence of the mode structure on comb generation using a model of two nonlinearly coupled phonon modes. The model predicts that there is only one region within the amplitude-frequency space where combs exist, and this region is a subset of the Arnold tongue that describes a 2:1 autoparametric resonance between the two modes. In addition, the location and shape of the comb region are analytically defined by the resonance frequencies, quality factors, mode coupling strength, and detuning of the driving force frequency from the mechanical resonances, providing clear conditions for comb generation. These results enable comb structure engineering for applications in areas as broad as sensing, communications, quantum information science, materials science, and molecular science.

<https://doi.org/10.1063/5.0025314>

Optical frequency combs have received considerable interest due to the stable broadband comb structure that can be generated, which has been a powerful tool in many applications, including optical clocks, spectroscopy, and microwave frequency synthesis.^{1,2} Like optical resonators, mechanical resonators have also been shown to be capable of generating equally spaced vibrational frequencies due to mechanical mixing and mode coupling.^{3–14} Early demonstrations^{3–6} revealed that by electrically driving coupled mechanical resonators or multiple modes in a single resonator using multiple drive frequencies simultaneously, a comb-like structure can be generated in the frequency domain. More recently, it was shown that a phononic frequency comb with a well-defined frequency structure can be generated with a single mechanical resonator that is driven with a single frequency.⁷ In this case, length extensional and flexural vibration modes are coupled through mechanical nonlinearities, providing a mechanism for mode coupling that generates phononic frequency combs when the amplitudes of the coupled modes saturate. Additional experimental observations of phononic frequency combs with a single drive frequency have since been reported that support the results in Ref. 7, including comb generation in a nanomechanical beam resonator,⁸ a coupled translational-rotational resonator,¹¹ and a membrane resonator.¹² The parametric mode coupling seen in Refs. 7–16 provides a path for engineering the comb structure and will likely find

applications in sensing, communications, and quantum information science, similar to optical frequency combs. In addition, this phenomenon of phononic combs could be exploited in material and molecular sciences, for instance, in the investigation of nonlinear phononics.^{17,18}

Despite the growing number of experimental observations of phononic frequency combs in mechanical resonators, it is still largely unclear how the resonance frequencies and quality factors of the interacting modes influence the generation and properties of the comb. The Fermi–Pasta–Ulam framework has previously been used to prove that a comb can be generated with a single drive frequency for a mechanical coupled-mode system.¹⁹ This analysis presented time-domain results that show that the comb can be phase coherent and that generation can be achieved through a wide range of nonlinearities and the number of coupled modes. More recently, a nonlinear friction mechanism has been shown analytically to be capable of generating a comb using just a single vibrational mode in a nanomechanical resonator.²⁰ In this paper, we analyze the effect of the resonance frequencies and quality factors of the coupled modes on the amplitude-frequency behavior of the comb. We apply the slowly varying envelope approximation to two coupled mechanical modes with a 2:1 autoparametric resonance and derive analytical existence conditions for phononic frequency combs. Using the derived existence conditions, the position and shape of the comb region relative

to resonance are also presented. This analysis provides guidelines for tailoring phononic frequency combs in mechanical resonators.

The generation of phononic frequency combs in the mechanical resonator described in Refs. 7, 9, 10, and 13 and shown schematically in Fig. 1 involves two steps. First, mode 1, which is a length extensional vibration mode, excites mode 2, which is a flexural vibration mode, when increasing the drive amplitude F above a certain threshold, i.e., above the red lines in Fig. 2. Second, mode 2 feeds back into mode 1 until the amplitudes of both modes oscillate and there is a continuous exchange of energy between the two modes. This is similar to a phenomenon found in optical parametric oscillators (OPO) where the idler is generated from the pump by increasing the pump power over a threshold.^{21,22} When further increasing F , modes 1 and 2 experience a temporal oscillation, similar to the slow time scale in Kerr combs. This corresponds to a Hopf bifurcation of two eigenmodes that are symmetric to the real axis. These eigenmodes transition from stationary to time-varying amplitude for specific drive, or pump, conditions, resulting in phononic frequency combs. This behavior is described by two coupled phonon modes with quadratic coupling nonlinearities and a 2:1 autoparametric resonance. The coupling is a result of a nonlinear strain relationship between the length-extensional and flexural modes,²³ and the equations of motion can be written as

$$\ddot{x}_1 + 2\gamma_1\dot{x}_1 + \omega_1^2x_1 + \alpha_{22}x_2^2 = F\cos(\omega_D t), \quad (1)$$

$$\ddot{x}_2 + 2\gamma_2\dot{x}_2 + \omega_2^2x_2 + \alpha_{12}x_1x_2 = 0. \quad (2)$$

Here, ω_1 and ω_2 are the resonance frequencies, where $\omega_1 \approx 2\omega_2$, γ_1 , and γ_2 are the damping rates, and $\alpha_{22}x_2^2$ and $\alpha_{12}x_1x_2$ are the nonlinear coupling terms. This system is driven by $F\cos(\omega_D t)$, where F is the drive amplitude and ω_D is the drive frequency. The coefficients α_{12} and α_{22} are part of the Fermi–Pasta–Ulam framework. Note: considering our experimental results,⁷ we assume the energy functional of the form $x_1x_2^2$ that is necessary and sufficient to generate phononic combs. However, in real experimental systems, the terms x_1^3 , x_2^3 , and $x_2x_1^2$ need to be added to accurately address the quantitative details. Specifically, the Duffing, or third-order, nonlinearity was not included in Eqs. (1) and (2) since experimental results showed the existence of phononic frequency combs before the Duffing nonlinearity had an effect on the frequency response.⁷ Furthermore, this analysis is focused

on existence conditions rather than accurate prediction of the comb amplitude. Solutions for x_j are assumed to be $x_j = (u_j e^{i\omega_D t} + u_j^* e^{-i\omega_D t})/2$ for $j = 1, 2$, where u_j are slowly varying envelopes.^{24,25} After substituting these solutions into Eqs. (1) and (2), the equations of motion can then be written in terms of the complex amplitudes, u_j ,

$$\ddot{u}_1 + [2\gamma_1 + 2i\omega_D]\dot{u}_1 + \left[(\omega_1^2 - \omega_D^2) + 2i\gamma_1\omega_D\right]u_1 + \alpha_{22}\frac{u_2^2}{2} = F, \quad (3)$$

$$\ddot{u}_2 + [2\gamma_2 + i\omega_D]\dot{u}_2 + \left[\left(\omega_2^2 - \frac{\omega_D^2}{4}\right) + i\gamma_2\omega_D\right]u_2 + \frac{\alpha_{12}}{2}u_1u_2^* = 0. \quad (4)$$

The generation of phononic frequency combs is indicated by the periodic modulation of the complex amplitudes u_j , where the modulation is slow compared to the carrier frequencies, resulting in pulsing between the two modes. In order to study these slow dynamics, the appropriate assumptions for the slowly varying envelope approximation are applied to Eqs. (3) and (4) (see the [supplementary material](#) for details on all derivations), providing two first-order differential equations that describe the normalized amplitudes of the two modes, ψ_1 and ψ_2 , when driven by a single frequency near the resonance of mode 1 (i.e., $\omega_D \approx \omega_1$),

$$\frac{\partial\psi_1}{\partial\tau} = -if - (1 + i\Delta_1)\psi_1 + i\psi_2^2, \quad (5)$$

$$\frac{\partial\psi_2}{\partial\tau} = -(\gamma_{21} + i\Delta_2)\psi_2 + 2i\psi_1\psi_2^*. \quad (6)$$

Here, $\tau = \gamma_1 t$, $f = \frac{\alpha_{12}}{8\gamma_1\omega_D} F$, $\gamma_{21} = \frac{\gamma_2}{\gamma_1}$, $\Delta_1 = \frac{\omega_D - \omega_1}{\gamma_1}$, $\Delta_2 = \frac{\omega_D - 2\omega_2}{2\gamma_1}$, $\psi_1 = \frac{\alpha_{12}}{4\gamma_1\omega_D} u_1$, and $\psi_2 = \frac{\sqrt{\alpha_{12}\alpha_{22}}}{4\gamma_2\omega_D} u_2$. To understand the conditions for comb generation within these slow dynamics, the stationary points have been investigated. Assuming steady-state conditions (i.e., $\frac{\partial\psi_1}{\partial\tau} = \frac{\partial\psi_2}{\partial\tau} = 0$), Eqs. (5) and (6) have two sets of stationary points: (ψ_{1L}, ψ_{2L}) and (ψ_{1P}, ψ_{2P}) . The first set is $\psi_{1L} = -f/(-j + \Delta_1)$, $\psi_{2L} = 0$. These stationary points are stable when f is small and provide the same expected amplitudes as the case where Eqs. (1) and (2) are linear (i.e., $\alpha_{12} = \alpha_{22} = 0$). The second set of stationary points, ψ_{1P} and ψ_{2P} , are defined by the following quadratic relationship:

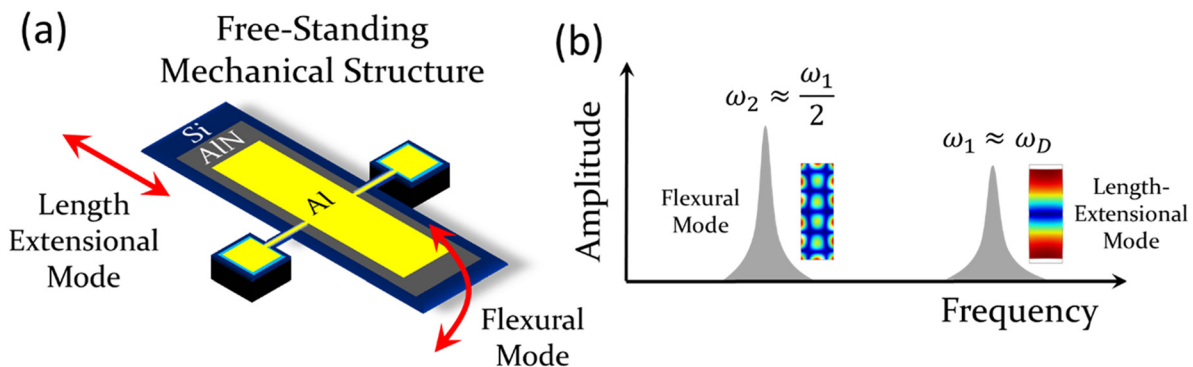


FIG. 1. Micromechanical resonator and phononic frequency comb concept. (a) Micromechanical resonator design used in Ref. 7 to generate phononic frequency combs. A length-extensional mode couples to a flexural mode through a nonlinear strain relationship. (b) Visual description of the mode coupling concept that results in phononic frequency combs, showing two modes where the resonance frequency of one mode is near double that of the other mode.

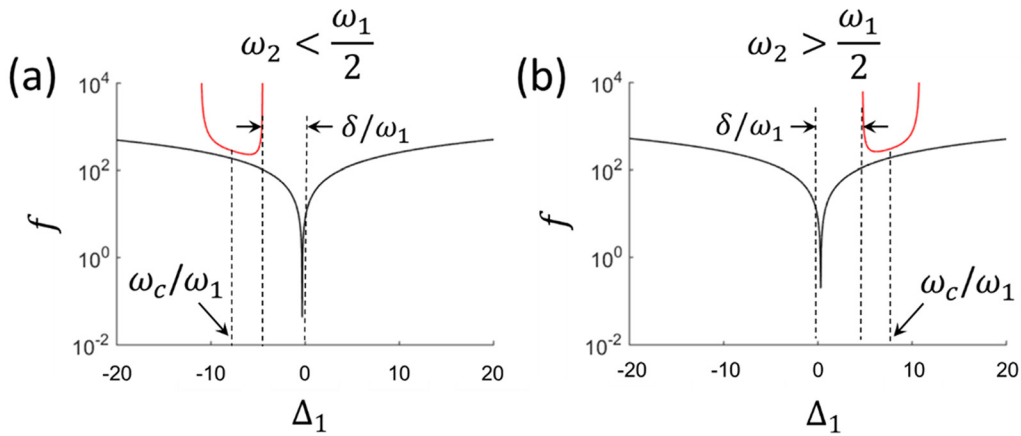


FIG. 2. Regions for parametric resonance (above the black line) and phononic frequency combs (above the red line) as a function of drive amplitude and frequency and the relative values of ω_1 and ω_2 . That is, the drive conditions above the black line lead to parametric modal coupling and the drive conditions above the red line lead to phononic frequency combs. The existence bounds for both red-detuned resonances (a) and blue-detuned resonances (b) are shown, where the detuning is for ω_2 relative to ω_1 . System parameters: (a) $\frac{\omega_1}{2\pi} = 3.86$ MHz, $Q_1 = 1000$, $\frac{\omega_2}{2\pi} = 1.9$ MHz, and $Q_2 = 10$; (b) $\frac{\omega_1}{2\pi} = 3.86$ MHz, $Q_1 = 1000$, $\frac{\omega_2}{2\pi} = 1.96$ MHz, and $Q_2 = 10$.

$$|\psi_{2P}|^4 + (\gamma_{21} - \Delta_1 \Delta_2) |\psi_{2P}|^2 + \frac{1}{4} (1 + \Delta_1^2) (\gamma_{21}^2 + \Delta_2^2) - f^2 = 0 \quad (7)$$

and $|\psi_{1P}|^2 = (\gamma_{21}^2 + \Delta_2^2)/4$. When ψ_{1P} and ψ_{2P} are stable stationary points, there is a 2:1 autoparametric resonance, or internal resonance, in which energy flows from mode 1 to mode 2, resulting in vibration of both modes with constant steady-state amplitude. Interestingly, ψ_{1P} is not a function of f because the amplitude is saturated and an increase in f will only increase ψ_{2P} . The stability of the slow dynamics, Eqs. (5) and (6), at ψ_{1P} and ψ_{2P} requires the discriminant of Eq. (7) be positive, $f \geq \frac{1}{2} |\gamma_{21} \Delta_1 + \Delta_2|$, which is shown in parameter space (f vs Δ_1) in Fig. 2 (black line). This condition sets the boundary for autoparametric resonance, often referred to as an Arnold tongue, where ψ_{1L} and ψ_{2L} are stable stationary points below the line and ψ_{1P} and ψ_{2P} may be stable above the line. The transition from ψ_{1L} and ψ_{2L} to ψ_{1P} and ψ_{2P} is a Hopf bifurcation.

In the case of autoparametric resonance, the oscillatory amplitudes ψ_1 and ψ_2 are at steady state (i.e., the amplitudes remain constant over time). However, in the case of phononic frequency combs, we have previously shown that the amplitudes, ψ_1 and ψ_2 , are modulated as a function of time such that periodic pulses are generated in the time domain, thereby resulting in frequency combs around the two modes.⁷ Therefore, Eqs. (5) and (6) are linearized about these stationary points such that small amplitude perturbations are defined as $\delta\psi_1$ and $\delta\psi_2$ and $\psi_1 \equiv \psi_{1P} + \delta\psi_1$ and $\psi_2 \equiv \psi_{2P} + \delta\psi_2$. Substituting into Eqs. (5) and (6) and applying steady-state conditions, $\frac{\partial\psi_1}{\partial\tau} = \frac{\partial\psi_2}{\partial\tau} = 0$, the linearized dynamics can be written as follows:

$$\frac{\partial\delta\psi_1}{\partial\tau} = -(1 + i\Delta_1)\delta\psi_1 + 2i\psi_{2P}\delta\psi_2, \quad (8)$$

$$\frac{\partial\delta\psi_2}{\partial\tau} = -(\gamma_{21} + i\Delta_2)\delta\psi_2 + 2i\psi_{1P}\delta\psi_1^* + 2i\psi_{2P}^*\delta\psi_1. \quad (9)$$

In order to study the stability of the linearized dynamics, it is assumed that $\delta\psi_1 = b_1 e^{\lambda\gamma_1 t}$, $\delta\psi_1^* = b_2 e^{\lambda^* \gamma_1 t}$, $\delta\psi_2 = b_3 e^{\lambda\gamma_2 t}$, and $\delta\psi_2^* = b_4 e^{\lambda^* \gamma_2 t}$, and modulations $\delta\psi_1$ and $\delta\psi_2$ can only grow in strength if λ is both

real and positive. After applying the Routh–Hurwitz criterion²⁶ to analyze the stability of the linearized dynamics, Eqs. (8) and (9), we obtain the following condition:

$$|\psi_{2P}|^2 \geq -\frac{\gamma_{21}(1 + \Delta_1^2)[1 + \Delta_1^2 + 4\gamma_{21}(1 + \gamma_{21})]}{4(1 + \gamma_{21})^2(1 + \Delta_1^2 + 2\gamma_{21} + 2\Delta_1\Delta_2)}. \quad (10)$$

This condition dictates the minimum value of $|\psi_{2P}|^2$ that is required for non-zero values of $\delta\psi_1$ and $\delta\psi_2$. Only such non-zero amplitude modulations can ensure the generation of side-bands in the frequency domain, which in turn yields the frequency comb spectra. Hence, the energy exchange between modes 1 and 2 should be significant enough to enhance the value of $|\psi_{2P}|$ in order to generate frequency combs. Similar to the autoparametric resonance, the transition from stable amplitudes to amplitude modulation is also a Hopf bifurcation.

Since $|\psi_{2P}|^2$ is always positive (i.e., $|\psi_{2P}|$ is real), we obtain a boundary condition for the existence of phononic frequency combs as $2\Delta_1\Delta_2 \leq -(1 + \Delta_1^2 + 2\gamma_{21})$. This boundary forms the subset of the region of autoparametric resonance, $f \geq \frac{1}{2} |\gamma_{21} \Delta_1 + \Delta_2|$, as shown in Fig. 2, where the red line represents the threshold for instability of the linearized dynamics. While this analysis cannot prove that comb generation is the only dynamic behavior found within this instability bound, the frequency dependence of phononic frequency combs in experimental results⁷ matches with the analytical evidence that the existence zone of phononic frequency combs is bounded in drive frequency. Figure 2 shows that the phononic combs exist in the red-detuned and blue-detuned sides of driven mode 1 for $\omega_2 < \frac{\omega_1}{2}$ and $\omega_2 > \frac{\omega_1}{2}$, respectively, for the presented model.

In order to verify that this bounded region describes the conditions for phononic frequency combs, we conducted numerical simulations of Eqs. (5) and (6) within this region. Figure 3 shows typical simulation results for mode amplitudes. The time domain responses [Figs. 3(a) and 3(b)] exhibit periodic oscillations and the corresponding fast Fourier transforms (FFT) [Figs. 3(c) and 3(d)] clearly demonstrate the existence of frequency combs.

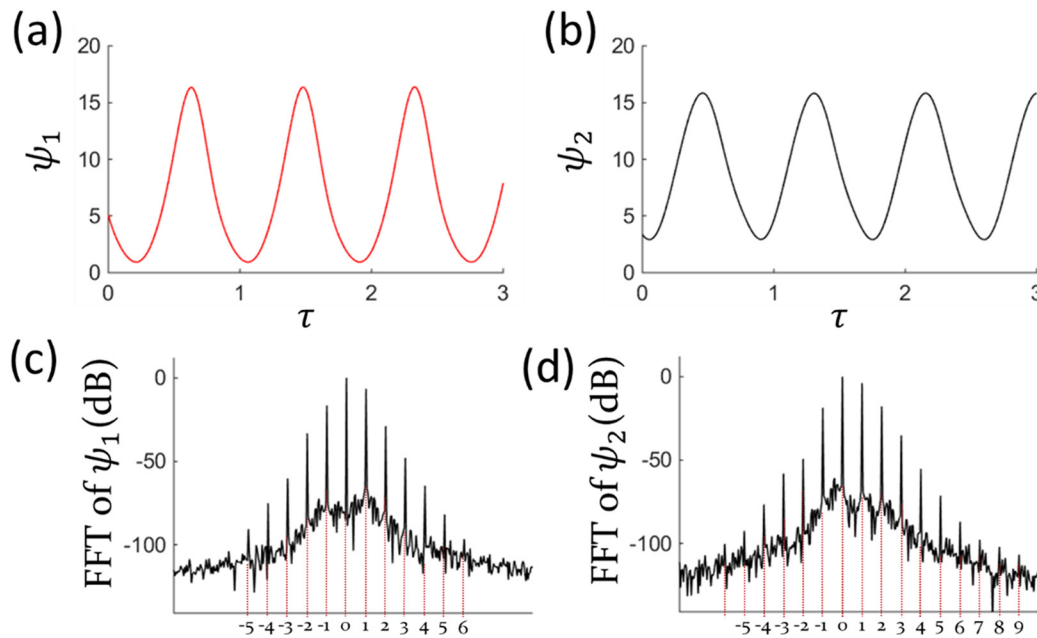


FIG. 3. Numerical simulation results for the mode amplitudes, Eqs. (5) and (6), within the phononic frequency comb boundary. Simulation parameters: $\Delta_1 = 5$; $\kappa = -9$; $\Delta_2 = \frac{\Delta_1}{2} + \kappa$; $\gamma_{21} = 1$; $f = 20$. (a) and (b) Time domain responses. (c) and (d) Corresponding fast Fourier transforms (FFT) showing the existence of phononic frequency combs.

Having established a description of the region in which combs can exist, we now investigate how the resonance frequencies and quality factors of modes 1 and 2 affect the location and shape of this region relative to the boundary describing the Hopf bifurcation to autoparametric resonance. To this end, the existence condition, Eq. (10), is considered. From the resulting boundary line, the parameter $\omega_c = \frac{1}{2}(\omega_{D,min} + \omega_{D,max})$ is defined as the center frequency of the comb region (Fig. 2) (see the [supplementary material](#) for definitions of $\omega_{D,max}$ and $\omega_{D,min}$). It has been derived in the [supplementary material](#) such that $\omega_c = \frac{1}{4}(3\omega_1 + 2\omega_2)$, with $\omega_2 \approx \frac{\omega_1}{2}$. For any value of ω_2 , the threshold for autoparametric resonance is always minimum when ω_D equals ω_1 . We now want to understand the minimum detuning from ω_1 that is required to excite phononic frequency combs. We know that phononic combs only exist in a specific frequency band. Depending on whether $\omega_2 > \frac{\omega_1}{2}$ or $\omega_2 < \frac{\omega_1}{2}$, ω_1 will be closer to either the left or right edge of phononic comb boundary. The difference between ω_1 and the edge of the existence boundary for combs corresponds to the minimum detuning that is required for generating frequency combs, which is $\delta = |\omega_{D,edge} - \omega_1| = \frac{\omega_1}{\sqrt{2Q_1Q_2}}$. By increasing the quality factors, Q_1 and Q_2 , δ is reduced, which in turn reduces the drive amplitude threshold for generating phononic combs. In other words, higher gain in the phononic combs can be obtained for smaller δ . This analysis also shows that phononic combs can be generated only if the quality factor Q_2 is set above a critical value of $Q_{2,c} = \frac{2}{Q_1} \left(1 - \frac{2\omega_2}{\omega_1}\right)^{-2}$, as shown in Fig. 4(a). The system parameters used in Fig. 4 were selected based on the experimental results in Ref. 7 so that the connection between the quality factors can be more easily understood. The frequency range R corresponding to the existence band of phononic combs is found to increase with Q_2 as

$R = \left|\omega_2 - \frac{\omega_1}{2}\right| - \left(\frac{\sqrt{2}\omega_1}{\sqrt{Q_1Q_2}}\right)$, which then asymptotes at $\left|\omega_2 - \frac{\omega_1}{2}\right|$ for large values of Q_2 . Similar to Q_2 , there also exists a critical value for $\left|\omega_2 - \frac{\omega_1}{2}\right|$, which is $g = 2\omega_1 \sqrt{\frac{2}{Q_1Q_2}}$. For $\left|\omega_2 - \frac{\omega_1}{2}\right| > g$, the frequency range R scales linearly with $\left|\omega_2 - \frac{\omega_1}{2}\right|$, as shown in Fig. 4(b). The above conditions can be used to design mechanical resonators that have a sufficient quality factor and placement of resonance frequencies to systematically generate phononic frequency combs.

Equation (10) shows that there is only one boundary zone for phononic frequency combs in a two-mode system, which either lies on the red-detuned or blue-detuned side of mode 1 (i.e., either $\omega_D < \omega_1$ or $\omega_D > \omega_1$). There is an interesting discrepancy between this model and the experimental results shown in Ref. 7. These results show that there are two boundary zones for phononic frequency combs and these zones lie on both sides of the resonance frequency (i.e., $\omega_D < \omega_1$ and $\omega_D > \omega_1$). The mode shapes for these two regions have been measured, as shown in Ref. 7, revealing that the mode coupling on either side of resonance is with two different modes. Referring to these as modes 2 and 3, the boundary zone that corresponds to $\omega_D < \omega_1$ can be explained by coupling between modes 1 and 2 and the zone corresponding to $\omega_D > \omega_1$ is due to coupling between modes 1 and 3. Hence, independently coupling a driven mode 1 to two different phonon modes leads to two bands of phononic frequency combs. Equation (10) can be directly employed to capture this more complex behavior, where the existence boundary for phononic combs resulting from the interactions of mode 1 and mode 2 is $2\Delta_1\Delta_2 \leq -(1 + \Delta_1^2 + 2\gamma_{21})$ and between modes 1 and 3 is $2\Delta_1\Delta_3 \leq -(1 + \Delta_1^2 + 2\gamma_{31})$.

In summary, this paper derives the existence conditions for phononic frequency comb generation with two coupled phonon modes in terms of drive frequency and amplitude. Using the boundary

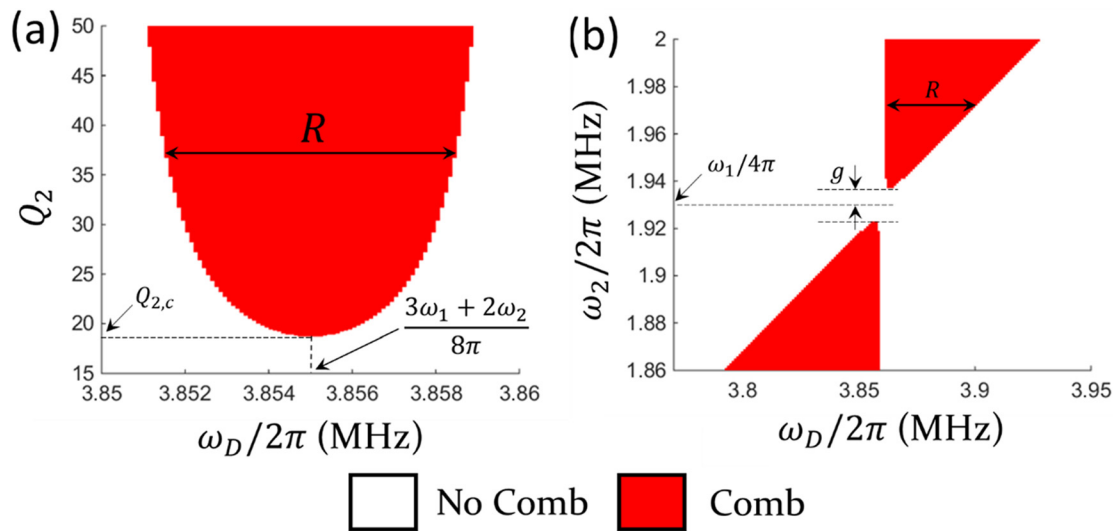


FIG. 4. Regions for generation of phononic frequency combs. (a) Quality factor of mode 2 vs drive frequency. (b) Resonance frequency of mode 2 vs drive frequency. System parameters: (a) $\frac{\omega_1}{2\pi} = 3.86$ MHz, $Q_1 = 4000$, and $\frac{\omega_2}{2\pi} = 1.92$ MHz and (b) $\frac{\omega_1}{2\pi} = 3.86$ MHz, $Q_1 = 4000$, $Q_2 = 50$.

conditions, we investigated the influence of modal properties, including the quality factors and resonance frequencies of interacting modes on the conditions for comb generation. These include critical modal frequency separation, critical quality factors, and critical detuning that are required to produce a phononic frequency comb. For a system of two coupled phonon modes, the analysis revealed that there is only one existence zone for phononic combs. However, by correlating these analytical results with published experimental results, distinct existence boundaries of phononic frequency combs can be generated by independently coupling a driven mode with several other phonon modes. The results of this work will accelerate the development of mechanical devices with enhanced phononic comb properties for their applications in physical sciences.

See the [supplementary material](#) for the derivations of existence conditions of phononic frequency combs.

DATA AVAILABILITY

The data that support the findings of this study are available from the corresponding author upon reasonable request.

REFERENCES

- ¹S. T. Cundiff and J. Ye, *Rev. Mod. Phys.* **75**, 325 (2003).
- ²T. J. Kippenberg, R. Holzwarth, and S. A. Diddams, *Science* **332**, 555 (2011).
- ³A. Erbe, H. Krömmmer, A. Kraus, R. H. Blick, G. Corso, and K. Richter, *Appl. Phys. Lett.* **77**, 3102 (2000).
- ⁴R. B. Karabalin, M. C. Cross, and M. L. Roukes, *Phys. Rev. B* **79**, 165309 (2009).
- ⁵I. Mahboob, Q. Wilmart, K. Nishiguchi, A. Fujiwara, and H. Yamaguchi, *Appl. Phys. Lett.* **100**, 113109 (2012).
- ⁶I. Mahboob, R. Dupuy, K. Nishiguchi, A. Fujiwara, and H. Yamaguchi, *Appl. Phys. Lett.* **109**, 073101 (2016).
- ⁷A. Ganesan, C. Do, and A. Seshia, *Phys. Rev. Lett.* **118**, 033903 (2017).
- ⁸M. J. Seitner, M. Abdi, A. Ridolfo, M. J. Hartmann, and E. M. Weig, *Phys. Rev. Lett.* **118**, 254301 (2017).
- ⁹A. Ganesan, C. Do, and A. Seshia, *Appl. Phys. Lett.* **112**, 021906 (2018).
- ¹⁰A. Ganesan, C. Do, and A. Seshia, *Phys. Rev. B* **97**, 014302 (2018).
- ¹¹D. A. Czaplewski, C. Chen, D. Lopez, O. Shoshani, A. M. Eriksson, S. Strachan, and S. W. Shaw, *Phys. Rev. Lett.* **121**, 244302 (2018).
- ¹²M. Park and A. Ansari, *J. Microelectromech. Syst.* **28**, 429 (2019).
- ¹³A. Ganesan and A. Seshia, *Sci. Rep.* **9**, 9452 (2019).
- ¹⁴S. Hourii, D. Hatanaka, M. Asano, and H. Yamaguchi, *Phys. Rev. Appl.* **13**(1), 014049 (2020).
- ¹⁵R. Singh, A. Sarkar, C. Guria, R. J. Nicholl, S. Chakraborty, K. I. Bolotin, and S. Ghosh, *Nano Lett.* **20**(6), 4659–4666 (2020).
- ¹⁶M. Goryachev, S. Galliou, and M. E. Tobar, *Phys. Rev. Res.* **2**(2), 023035 (2020).
- ¹⁷M. Först, C. Manzoni, S. Kaiser, Y. Tomioka, Y. Tokura, R. Merlin, and A. Cavalleri, *Nat. Phys.* **7**(11), 854 (2011).
- ¹⁸D. M. Juraschek, Q. N. Meier, and P. Narang, *Phys. Rev. Lett.* **124**, 117401 (2020).
- ¹⁹L. S. Cao, D. X. Qi, R. W. Peng, M. Wang, and P. Schmelcher, *Phys. Rev. Lett.* **112**, 075505 (2014).
- ²⁰M. I. Dykman, G. Rastelli, M. L. Roukes, and E. M. Weig, *Phys. Rev. Lett.* **122**, 254301 (2019).
- ²¹J. A. Giordmaine and R. C. Miller, *Phys. Rev. Lett.* **14**, 973 (1965).
- ²²J. J. Baumberg, P. G. Savvidis, R. M. Stevenson, A. I. Tartakovskii, M. S. Skolnick, D. M. Whittaker, and J. S. Roberts, *Phys. Rev. B* **62**, R16247 (2000).
- ²³C. van der Avoort, R. van der Hout, and J. Hulshof, *Physica D* **240**, 913 (2011).
- ²⁴K. D. Shaw, *Opt. Commun.* **85**, 191 (1991).
- ²⁵H. Leblond and D. Mihalache, *Phys. Rep.* **523**, 61 (2013).
- ²⁶B. C. Kuo, *Automatic Control Systems* (Prentice-Hall, New Jersey, 1995).